Ocean Sci. Discuss., 9, 3521–3566, 2012
www.ocean-sci-discuss.net/9/3521/2012/
doi:10.5194/osd-9-3521-2012


Ocean Science Discussions



# Assymmetric eddy populations in adjacent basins – a high resolution numerical study of the Tyrrhenian and Ligurian Seas

**R. M. A. Caldeira[1,2], X. Couvelard[2], E. Casella[3], and A. Vetrano[4]**

[1]CIIMAR-Interdisciplinary Centre of Marine and Environmental Research, Rua dos Bragas, 289, 4050-123 Porto, Portugal
[2]CCM-Center for Mathematical Sciences, University of Madeira, Campus da Penteada, 9000-390, Funchal, Madeira, Portugal
[3]CIMA Research Foundation, Via Armando Magliotto, 2-17100 Savona, Italy
[4]CNR-ISMAR, Institute of Marine Science, Forte Santa Teresa, Pozzuolo di Lerici, 19032 La Spezia, Italy

Received: 28 September 2012 – Accepted: 22 October 2012 – Published: 12 November 2012

Correspondence to: R. M. A. Caldeira (rcaldeira@ciimar.up.pt)

Published by Copernicus Publications on behalf of the European Geosciences Union.

## Abstract

A high-resolution ocean circulation modelling system forced with a high-resolution numerical wind product was used to study the mesoscale and sub-mesoscale eddy population of the North-Western Mediterranean Sea, contrasting eddy-activity between the Tyrrhenian and Ligurian sub-basins. Numerical solutions reproduced some of the known regional dynamics, namely the occurrence and oceanic implications of Mistral events, the convective cell leeward of the Gulf of Lion, as well as the Balearic frontal system. Calculated transport across the Corsica Channel followed a similar trend, when compared to the transport computed from a moored current meter. The analysis of the results showed that surface eddy activity is mostly confined to the boundary-currents, whereas in the deeper layers most eddies are concentrated on the central-deeper part of the basins. The Liguro-Provençal basin shows a much higher concentration of intermediate and deep-water eddies, when compared to the Tyrrhenian basin. Sub-mesoscale surface eddies tend to merge and migrate vertically onto intermediate waters. Intense eddy activity in the boundary-current surrounding the Liguro-Provençal Gyre, concentrate high-productivity, manifested by higher concentrations of mean sea surface chlorophyll, in the central part of the gyre, defined herein as the Ligurian Productive Pool (LPP). On average, the Tyrrhenian was mostly oligotrophic except for a small productive vortice in the south-eastern (leeward) side of Corsica. The transport in the Tyrrhenian Gyre, and across the basin is one order of magnitude higher than the transport calculated for the Liguro-Provençal basin. A high concentration of eddies in the passage between the Balearic Archipelago and Sardinia suggests retention and longer residence times of nutrient rich water in the "Ligurian pool", compared to a "fast draining" Tyrrhenian basin. Previous studies support the cyclonic gyre circulation generated in the Liguro-Provençal basin but more studies are needed to address the surface and deep mesoscale activity of the Tyrrhenian basin.

## 1 Introduction

The Mediterranean Sea is composed by a series of semi-enclosed basins, connected via straits and passages. These sub-basins are often deep in their central part, and surrounded by a narrow continental shelf. Several authors depicted these sub-basins as important contributors to the formation of waters masses, where the different atmospheric and oceanic dynamics at the sub-basin scales may lead to the generation of a thermohaline driven circulation. These water masses spill into the central part of the Mediterranean and eventually find their way into the Atlantic Ocean (e.g. Millot, 1999; Zavatarelli and Mellor, 1995; Pinardi and Masetti, 2000; Millot and Taupier-Letage, 2005; Robinson et al., 2001).

At the sub-basin scales the existence of a boundary-current at the shelf edge is commonly described. Topographically-induced or baroclinic-induced instabilities of this boundary-current can generate strong eddy activity (Santoleri et al., 1983; Marullo et al., 1994; Baey et al., 1995; Sammari et al., 1995; Gasparini et al., 1999; Robinson et al., 2001; Echevin et al., 2003). Despite many efforts that have been made to study the Mediterranean and sub-basin dynamics, the spatial and temporal distribution of mesoscale and sub-mesocale eddy activity has been hard to capture with remote sensing products, and the region is rather large to allow for a basin-wide in situ sampling campaign. Considering that the Rossby deformation radius (Rd) in this region varies from 10 to 14 km, four times smaller than the values for most of the worlds ocean, the numerical study of mesoscale variability requires much finer resolutions. Pre-gridded AVISO altimetry data has a threshold of 40 km radius, compromising an accurate eddy detection (Chelton et al., 2011), thus much of the mesoscale dynamics within these basins remains undersampled. Data from passive satellite sensors such as SeaWiFS and MODIS are intermittently available since they are highly affected by clouds. Fine-resolution numerical studies are expensive and until very recently not affordable for most research teams. Furthermore, since ocean surface dynamics is highly influenced by wind forcing, high-resolution wind products also need to be considered in sub-basin





OSD
9, 3521–3566, 2012

scale studies of the Mediterranean Sea (Small et al., 2012). Notwithstanding these limitations, several studies have suggested the importance of sub- and mesoscale eddy activities in these basins, often combining observations with numerical modeling (Millot, 1999; Sammari et al., 1995; Robinson et al., 2001; Echevin et al., 2003; Vetrano, 2004). To the best of our knowledge, no previous study has address the depth distribution of (sub)mesoscale eddy features, nor have the comparative study of Ligurian and Tyrrhenian eddy populations been performed previously.

Figure 1 represents the main sub-basins of the Mediterranean Sea. The two sub-basins of the Western Mediterranean (Liguro-Provençal and Tyrrhenian), are separated by the islands of Sardinia and Corsica (Fig. 1). The literature suggests the occurrence of several surface currents and strong thermohaline processes occurring in these two basins. The existence of a boundary-current is mainly identified as being the Tyrrhenian (also known as Bifurcated Tyrrhenian) Current (TC), which runs on the Italian continental shelf (Millot, 1999); the Eastern Corsica Current is a bifurcation of the TC and runs northwards, as suggested by its name, along the Eastern side of Corsica (Millot, 1999; Astraldi and Gasparini, 1992; Vignudelli et al., 2000; André et al., 2005); after turning around the southern side of Sardinia, this current is often designated as the WCC – Western Corsica Current (Taupier-Letage and Millot, 1986; Millot, 1999; Astraldi and Gasparini, 1992; André et al., 2005). The Liguro-Provençal Current (LPC) has been observed to run on the northern part of the basin (Albérola et al., 1995; Conan and Millot, 1995; Sammari et al., 1995; Robinson et al., 2001; André et al., 2005; Birol et al., 2010). The Balearic Current (BC) has been proposed as being an important part of the South-West Liguro-Provençal basin south-west circulation (Font et al., 1988; Millot, 1999; Pinot et al., 1995; Salat, 1995; Robinson et al., 2001). The Balearic Current is known to cross the basin to join the Western Corsica Current (e.g. Castellón et al., 1990). The Algerian Current (AC) flows along the North African shelf and is in connection with the TC (e.g. Millot, 1999). Sub- and mesoscale eddies are expected to spin off these boundary-currents, playing an important role on the transport of water in and out of these basins. The basin-scale circulation is represented in a cartoon form in Fig. 1.

The passage between the Balearic Islands and Sardinia is known to lodge strong eddy activity (Millot, 1999). In fact Fig. 2 (middle panel) shows strong mean kinetic energy in this region, suggesting persistent eddy activity.

The aim of the present work is to contribute to the discussion of the role of mesoscale eddy activity in the Mediterranean sub-basins, namely the Liguro-Provençal and Tyrrhenian basins. Despite their similar size and geographic configuration, their dynamics are different, thus with different implications to the mean biological productivity. After briefly reviewing the state-of-the-art in this introductory section, the methods used for data analysis and numerical computations are detailed in Sect. 2. In Sect. 3, after discussing the model representation of some of the known regional dynamics, results of the eddy population structure are interpreted and compared with previous findings. In Sect. 4 the main results are summarized.

## 2 Data and numerical analysis

### 2.1 Satellite data

The altimeter products used in this study were produced by Ssalto/Duacs and distributed by Aviso, with support from Cnes (http://www.aviso.oceanobs.com/duacs/) and used for Kinetic Energy (KE) computation. Surface velocities were computed from weekly merged products of Absolute Dynamic Topography (ADT), at 1/8° resolution on a Mercator projection. Maps are obtained by merging measurements from all available altimeter missions (Ducet et al., 2000). Combining data from different missions significantly improves the estimation of mesoscale signals (Pascual et al., 2007). The processed data considers up to 4 satellites at a given time, thus it has the best possible regional sampling. Furthermore, the period of the study (2009–2010), has one of the best altimetry coverage with a four-satellite constellation (Jason 1, Jason 2, Envisat and Cryostat). ADT is obtained adding along track Sea Level Anomaly to the Mean Dynamic Topography (Rio and Hernandez, 2004).

The Sea Surface Temperaure (SST) data have been developed and disseminated by the GOS ("Gruppo di Oceanografia da Satellite – ISAC, CNR"). The product is *GOS-L4HRfnd-MED-DTv1*. All GOS products are based on the measurements obtained by available satellite infrared sensors (AATSR, AVHRR, MODIS, SEVIRI). The Level-4 data provided by GOS-ISAC at CNR, represents the temperature at the base of the daily thermocline, at mid-night. The spatial resolution of this dataset is 1/16° Chlorophyll data were derived from the MODIS-Moderate Resolution Imaging Spectro-radiometer flying onboard of the Aqua platform. MODIS data has been processed by the Ocean Biology Processing Group (OBPG), at the Goddard Space Flight Center. Merged Level-3 chlorophyll products are being created routinely for daily, 8-day, monthly, seasonal and annual time periods, processed at a 9 km spatial resolution.

### 2.2 Current meter data

Within the Corsica Channel there is an underwater station at about 450 m depth, managed by CNR ISMAR – La Spezia, and located between the islands of Capraia and Corsica, at the sill of the channel. It continuously measures ocean currents and thermohaline properties of water masses at predetermined depths, for the monitoring of the surface and the intermediate circulation of the Mediterranean Sea, and the exchanges between the two adjacent basins (Tyrrhenian Sea and Ligurian Sea). The site has been active since 1985 and is now part of the CIESM Hydrochanges Programme (see http://www.ciesm.org/marine/programs/hydrochanges.htm). For the present paper data from 2009 and 2010 has been used to compute the total northward transport through the channel. Until March 2010 hourly velocity data at 4 discrete depths are available: 70 m, 125 m, 320 m and 415 m. The northward transport has been computed by multiplying velocity data with the corresponding areas of the section. Since March 2010 an Acoustic Doppler Current Profiler (ADCP, RDI WH Longrange) has been installed on the mooring, measuring velocity data with a 2-h interval onto 24 16-m-deep bins, from the bottom to the sea surface, allowing a much more accurate transport





OSD
9, 3521–3566, 2012

estimation. Nevertheless, in order to preserve coherence within the 2009–2010 time series, the ADCP data considered velocities at four discrete depths.

### 2.3 The ocean circulation modeling system

The Regional Ocean Modeling System (ROMS) (Shchepetkin, 2003; Shchepetkin and McWilliams, 2005) has been configured for the north western part of the Mediterranean Sea (Fig. 1). ROMS solves the primitive equations based on the Boussinesq approximation. In the Ligurian model solutions for 2009 and 2010, the model domain extends northward between 37.8° N to 44.5° N and eastward between 2° E to 16.5° E. The bottom topography is derived from a 30 arc-second resolution database GEBCO (available at http://www.gebco.net) and represented in Fig. 1. In the model version used herein, there are two open lateral boundaries: at 37.8° N and 2° E. In the Regional model the horizontal resolution was 1/32° is (3 km). At this resolution, the Rossby radius of deformation is resolved and consequently the model configuration is adequate to simulate (sub-)mesoscale structures in the whole Mediterranean and for different seasons (Grilli and Pinardi, 1998). The model grid has 35 vertical levels with vertical refinement near the surface to obtain a satisfactory representation of the surface layer. At the open lateral boundaries, the model is forced with temperature, salinity and velocity fields obtained from the MERCATOR product PSY2V3 (http://www.mercator-ocean.fr). MERCATOR, has an horizontal spatial resolution of 1/12°, with daily outputs. At the sea surface, ROMS was forced with the monthly mean climatology of heat and freshwater fluxes, derived from the Comprehensive Ocean-Atmosphere Data Set, COADS (da Silva et al., 1994). For the atmospheric momentum calculation, wind-stress was extracted from the Limited Area Model Italy (COSMO-I7) (Montani et al., 2003); a non-hydrostatic and fully compressible numerical weather prediction model, which is a regional version of the lokal model (Doms and Schättler, 2002) regularly used for operational and research applications. The COSMO-I7 three hourly solutions have a horizontal spatial resolution of 1/16°. Validation of the COSMO-I7 wind fields has been performed (Steppeler et al., 2003). As previously stated by several authors (Pinardi





OSD
9, 3521–3566, 2012

and Navarra, 1993; Molcard et al., 1998, 2002; Casella et al., 2011), to accurately represent the main features of the general circulation and the characteristics of the local circulations at the Mediterranean sub-basin scales, the use of high-frequency wind forcing is crucial. Accurate wind variability will correctly reproduce observed convection depths and formation rates, due to the intermittent and often violent nature of these phenomena in the region.

## 2.4 Eddy detection algorithm

In order to detect and track eddies from our numerical solution the "Vector Geometry-Based Eddy Detection Algorithm" (Nencioli et al., 2010) was applied to the ROMS and MERCATOR outputs. This algorithm represents an alternative to other existing approaches like Okubo–Weiss Parameter $W$ (Isern-Fontanet et al., 2004; Chelton et al., 2007), the wavelet analysis (Doglioli et al., 2007) and the winding angle method (Sadarjoen and Post, 2000; Chaigneau et al., 2008).

The "Vector Geometry-Based Eddy Detection Algorithm" is a method entirely based on geometrical characteristics of the flow field, it identifies eddies based on the shape or curvature of the instantaneous streamlines. The method is particularly appropriate for the analysis of eddy activity from high-resolution numerical experiments and/or altimetry data (Nencioli et al., 2010; Liu et al., 2012; Dong et al., 2012). Four parameters are defined: (i) the first parameter, ($a$), defines how many grid points in magnitude of $v$ (along the E–W axes) and $u$ (along the N–S axes) are checked; (ii) the second parameter, ($b$), defines the dimension, in terms of grid points, of the area used to define the local minimum of velocity; (iii) the third parameter, ($r$), is the number of grid point to define the initial area to compute eddy dimensions; concerning the eddy tracks, they are determined by comparing the eddy centers at successive time steps, starting from day one within a searching area; (iv) the fourth parameter, (rad), is the searching area. A complete description of all the parameters and tracking algorithm is detailed in Nencioli et al. (2010).





OSD
9, 3521–3566, 2012

After few sensitivity tests for the study region, the set of parameters was tuned to be a fixed values throughout the analysis ($a = 4$; $b = 3$; rad = 4; $r = 15$). Eddies with lifetime between 1–10 days and greater than 10 days were considered separately.

## 3 Results and discussion

### 3.1 Representation of the regional ocean dynamics

Comparing the mean Kinetic Energy (KE) fields computed from AVISO altimeter data, with MERCATOR (father model) and ROMS (child model), a strong KE activity appears in the same sub-regions (Fig. 2). The Liguro-Provençal boundary-current has high KE, as shown in all products. Strong KE activity is also shown in the Algerian coastal current region, in particular when comparing the MERCATOR solution with the AVISO merged product (this region is not included in ROMS model). Although less energetic, the surface signature of the Tyrrhenian coastal current, including its passage through the Sicily northern shelf region is well depicted. The Eastern and Western Corsica currents, and the Balearic current are also present but less energetic if compared to the other currents. In brief, strong KE is associated with the occurrence of these boundary-currents at the surface.

Another well-known process of the Western Mediterranean is the occurrence of the Mistral events, leeward of the Gulf of Lion (Millot, 1999; Small et al., 2012). Figure 3b shows the mean wind-stress (from 10 m winds) calculated from the COSMO-I7 atmospheric model, manifesting the persistence of these Mistral episodes during 2009. The mixed layer depth is expected to react to this heterogeneous wind forcing. In fact, leeward of the Gulf of Lion the regional model often reveals a much deeper mixed layer depth (MLD) than elsewhere (see Fig. 4). The MLD reached 150 m in the Liguro-Provençal basin whereas it remained shallower in the Tyrrhenian basin. There is some inter-annual variability and the vertical mixing is greater in 2010 than in 2009 (Fig. 4), nevertheless the main patterns are maintained.





OSD
9, 3521–3566, 2012

Eddy populations in adjacent basins

R. M. A. Caldeira et al.

Millot (1999) in a review of the ocean circulation of the Western Mediterranean Sea discussed several evidences that suggested the formation of WIW – Winter Intermediate Water in front of the Gulf of Lion, due to the occurrence of the wind-induced convective processes acting on the surface AW – Atlantic Water. There was also intense discussion on the transport of intermediate waters between the Liguro-Provençal and the Tyrrhenian basins, and the subsequent interaction which might occur with LIW – Levantine Intermediate Waters (coming from the Eastern Mediterranean), leading to the formation of particular water mass denominated as the TDW – Tyrrhenian Deep Water. Although our main goal is not to focus on the study of water mass formation, the intense eddy activity and their pathways across the basins does suggest that eddies might indeed play an important role on transport of individual "pools" of intermediate- and deep-water to and from neighboring basins. In the ROMS solutions, at the surface (0–10 m) and below 500 m a series of mesoscale eddies are frequently detected crossing the Sicily Channel. Perhaps the alleged intermittent across-basin transport of different water mass, referred by Millot (1999), is carried out by waters entrained in mesoscale eddies. Millot (1999), has also summarized the results from several in situ CTD campaigns in the Tyrrhenian basin suggesting that cascading events at the Tyrrhenian southern entrance are occurring down to $\sim 2000$ m, inducing strong deep mixing in this basin and thus weak transport of nutrients to the surface. As discussed bellow, on average the Tyrrhenian basin is oligotrophic; in contrast to a high productive Ligurian basin.

Small et al. (2012), studied the response of the Ligurian and Tyrrhenian Seas to a summer Mistral event (3 days) coupling an atmospheric model to an oceanic one. Their results showed that the use of high-resolution wind is crucial for the accurate representation of the wind stress induced by these events. Wind jets in this region are sensitive to orographic features, which are often missed in climatological and/or low-resolution products. The authors also argue for the contribution of extreme wind events for the maintenance of the basin scale gyre that is often observed in the





OSD
9, 3521–3566, 2012

Liguro-Provençal basin. This was also previously hypothesized by (Herbaut et al., 1997; Schroeder et al., 2008; Carniel et al., 2002; Poulain et al., 2012).

Testor and Gascard (2006), studied the cross basin spreading of post-convection water from the Gulf of Lion. Anticyclonic and cyclonic eddies were observed by SOFARGOS drifters traveling away from the source region. With a 5 km radius, these sub-mesoscale eddy features were also observed interacting with larger features in the Ligurian-Provençal Current, in the North Balearic front, and with Sardinian eddies (Testor and Gascard, 2003). Thus the authors concluded that the long-term behavior of these eddies represents an important part of the large scale thermohaline circulation, particularly regarding their alleged role in the transport of parcels of water across the basin (Testor and Gascard, 2005).

Also the mean SST reflects the effect of the asymmetric wind forcing (see Fig. 5b). On average, sea surface water temperature is 5–6 °C lower in the Liguro-Provençal basin than south of the passage between the Balearics and Sardinia and/or in the Tyrrhenian basin. In fact, a frontal system is formed between the inner and outer parts of the Liguro-Provençal basin. The persistence of the positive wind-stress induced by Mistral events might contribute to the formation and maintenance of a cyclonic gyre inside the Liguro-Pronveçal region. Cyclonic motion in turn tends to upwell colder and saltier waters from below. These upwelled cool waters are also persistent leeward of the southeast of Corsica and Sardinia, where positive wind-stress is also dominant. Small et al. (2012) has observed this feature as well, in relationship to the wind-stress leeward of southeastward side of Corsica Island. The mean SST calculated with the regional model shows similar patterns when compared to the mean SST measured by satellite data (Fig. 5b). ROMS simulates lower (1–2°) averaged SST than measured by satellite, even though the main patches of warm and cold water occur in similar regions, suggesting that the mesoscale dynamics are well represented by the model.

A time-series of moored currentmeter measurements in the Corsica Channel (its position is shown in Fig. 1), shows a good agreement between the 2009–2010 transport calculated from the model solutions and the one derived from the current meter dataset





OSD
9, 3521–3566, 2012

(Fig. 6). Calculated peaks of 1–2 Sv are corroborated by measured data. It is important to note that the Corsica Channel is a very narrow passage and considering the bathymetric smoothing characteristic of a sigma coordinate model, even at high resolution, the model extracted data are never at the same exact location and depth of the measured ones, nor it has the exact bathymetric characteristic of the moored location. Despite these limitations the model is representing well the variability of the measured transport through the Corsica Channel (Fig. 6).

Without claiming that the regional model is representing all of the dynamic aspects of the region, we are confident that the above results suggest that the main known processes of the Western Mediterranean are captured by the numerical solution. Thus, ROMS results will be used hereafter to study the sub- and mesoscale eddy populations in the Liguro-Provençal and Tyrrhenian basins. Hopefully this can lead us to further understand their role in the general circulation as well as their capacity to induce and to maintain biological productivity.

### 3.2 Eddy population distribution

Figure 7a shows the detected eddies (with lifetimes greater than 10 days), and their sea surface paths, for MERCATOR and ROMS solutions during the 2009–2010 study period. Despite the similarities, MERCATOR resolution (1/12°) together with the resolution of its wind-forcing product was insufficient to represent the strong occurrence of sub-mesoscale ($\ll$ Rd) eddy activity in the two basins. On the other hand, ROMS (1/32°) resolution, with its high-resolution wind-forcing product (COMSO-I7), revealed denser eddy activity both at the surface as well as at depth (Fig. 7a). The distribution of eddies at the surface is different from the eddy distribution at greater depths. At the surface (ROMS) eddies tend to aggregate at the boundary-currents, whereas in depths between 50–2000 m eddies are concentrated at the deepest part of the basins. Liguro-Provençal basin shows the occurrence of more eddies than the adjacent Tyrrhenian basin. The circulation on the deepest part of the Tyrrhenian basin is strong, i.e. 10 Sv. Although not shown here, eddy distribution in ROMS is similar between 0 and





OSD
9, 3521–3566, 2012

10 m depth, assuming a very similar aggregation pattern thereafter. In ROMS solutions, most of the surface eddies aggregated in the boundary current system, i.e. LPC, TC, ECC, WCC and BC (see Fig. 1). On the other hand, the deep eddies are concentrated at the deepest part of the basin. Both ROMS and MERCATOR solutions show a higher concentration of (sub)mesoscale eddies in the Liguro-Provençal basin than the adjacent Tyrrhenian basin. There is also a strong cluster of eddies in the passage between the Balearic Archipelago and Sardinia.

Analyzing in detail the eddy population several new details arise. When considering eddies with lifetimes between 1 and 10 days for the 2009–2010 period (0–2000 m), there are a total of 11 259 eddies detected for MERCATOR and 42630 for ROMS. Accounting for eddies with lifetimes greater than 10 days, the MERCATOR solution generates 2383 eddies, whereas the ROMS solution produces 6434 eddies, suggesting that in the first 10 days eddy merging and/or dissipation takes place.

The depth distribution shows similar general patterns in ROMS and MERCATOR for eddies with lifetimes greater than 10 days, thus model resolutions does not seem to affect mesoscale eddy distribution, except that the higher resolution model (ROMS) resulted in the generation of more eddies (see Fig. 8b). On the other hand, for eddies with life times between 1 and 10 days, where a great percentage of sub-mesoscale eddy activity emerges, the ROMS and MERCATOR depth distributions are different. The highest concentration of eddies occurred between the surface and 10 m, for the MERCATOR, whereas for ROMS the highest concentration of sub-mesoscale eddy activity is concentrated between 10–200 m, with fewer eddies at the surface (0 m). As mentioned previously, sub-mesoscale eddies are expected to merge and migrate vertically in the ROMS solutions, but not all these processes are resolved by the MERCATOR grid resolution (1/12°) (i.e. $\ll$ Rd).

The age of eddies in a depth distribution diagram shows that most eddies lived 15–60 days both in MERCATOR and ROMS solutions (Fig. 9b). Eddies that live longer (90–120 days) are mostly confined to the deeper layers. No eddies older than 360 days were detected. Short-lived anticyclones occurred in the intermediate layers (0–100 m),





OSD
9, 3521–3566, 2012

whereas most short-lived cyclones were found below 50 m. This depth eddy distribution also confirms the former conclusion that anticyclonic eddies were mostly dominant at the surface and intermediate waters; whereas cyclonic eddies dominate the deeper layers (200–2000 m).

Eddy maximum sizes are also asymmetrically distributed with depth (Fig. 10). Considering the ROMS solution for the two year period (2009–2010), smaller eddies (< 10 km), are detected at the surface, whereas sightly larger eddies (60–65 km), are found in the intermediate and deeper layers (200–500), for both cyclonic and anticyclonic. Below 1000 m eddy size distribution remains unchanged. The maximum and minimum sizes change gradually from the surface to the intermediate depths suggesting that most of the eddy-merging activity occurs at the surface with a subsequent growth to the intermediate layers. ROMS and MERCATOR (not shown) show similar size distribution patterns.

Demirov and Pinardi (2007) claimed that the formation and spreading of water masses in the Western Mediterranean Sea has a contribution from strong eddy activity in the region. Eddies of newly formed deep waters tend to merge and enlarge before their cross-basin travel. Legg and McWilliams (2001) already demonstrated that in horizontally homogenous surface forcing (such as the region in front of the Gulf of Lion), deep convection tends to be very localized with mesoscale vortices playing an important role in the formation and transport processes. The homogenization of the water column during violent mixing stages diminishes the Rossby deformation radius, thus favoring baroclinic instability of the flow and consequently eddy generation. Legg and McWilliams (2001), argue that in such events the flow during the first days and weeks after a deep convection event is expected to be dominated by relatively small eddies (e.g. sub-mesoscale), which tend to merge and enlarge with time. Merged and larger eddies are expected to migrate downwards, thus explaining the high concentration of larger eddies in the center of the Liguro-Provençal basin. Demirov and Pinardi (2007) also argue for the existence of a baroclinic instability cascade, which results from the conversion of the Available Mean Potential Energy (APEm) into Available

Potential Energy (APEe), which in turn is transformed into Eddy Kinetic Energy (EKE), as the dominant mechanism for eddy formation in the Algerian and Liguro-Provençal basins.

### 3.3 Theoretical and laboratory considerations

Several laboratory and theoretical studies have focused on the circulation of semi-enclosed basins. Often these idealized approaches study a highly simplified system; nevertheless their discussion herein can contribute to the general understanding of the complex dynamics as well as help guide future investigations.

Pedlosky et al. (1997), used laboratory and numerical experiments to expand on Godfrey original "island rule", by placing an island in the center of a closed circular basin (i.e. halved-cylinder). In the meridional case study, the "island" separated the two sub-basins, connected by passages at the north and southern ends, in a configuration similar to the Corsica and Sardinia Islands separating the Liguro-Provençal and the Tyrrhenian sub-basins. The mass Sverdrup transport around the central "island" thus became a discussion on the vorticity budget. In a linear quasi-geostrophic state, a Sverdrup Gyre developed on the eastern side of the "island" (i.e. analogous Tyrrhenian side), whereas on the western sub-basin the streamlines were parallel to the "island". As the nonlinearity of the circulation system increased the recirculation within the two sub-basins become increasingly asymmetric. In a strongly nonlinear case a second gyre appeared at the northwestern end (i.e. analogous to the Ligurian-Provençal Gyre).

Pedlosky et al. (1997) study has also considered the asymmetric wind stress effects on the basin circulation. Applying strong wind stress only to the western sub-basin (i.e. analogous to the strong influence of the Mistral events in Liguro-Provençal basin), apart from developing a boundary current around the basin, the fluid also started a secondary cyclonic circulation around the central-island (analogous to the ECC and WCC circulation around the Corsica–Sardinia), forming a western boundary layer asymmetric problem. In the latter case the circulation on the southeastern sub-basin was mainly composed of closed streamlines, whereas on the northwestern side the flow became unsteady and included the generation of eddies. A similar consequence is also observed in the Liguro-Provençal and Tyrrhenian basins, whereas the mean cyclonic circulation meanders around the Liguro-Provençal basin, in the Tyrrhenian basin the boundary-current appears "symmetric" (see discussion of the transport calculation below).

Despite the simplified assumptions of the "island rule" study, the similarities with the mean circulation patterns of the Liguro-Provençal and the Tyrrhenian basins are remarkable. Boundary currents (in this case WCC and ECC) embrace the central island in a cyclonic manner rounding the north and southern corners, while an outer Sverdrup Gyre (i.e. analogous to the joint effect of LPC and TC), continue to dominate the shelf-edge. Therefore, Pedlosky et al. (1997) idealized studies do suggest a relationship between the inner cyclonic circulation (around Corsica and Sardinia), and the outer boundary-current gyre, and that the asymmetric wind-stress might be playing an important role on the destabilization of the northwestern Liguro-Provençal sub-basin boundary circulation. Pedlosky et al. (1997), has also observed more eddy activity in the western unstable basin, compared to the eastern basin, analogous to asymmetric eddy population for the Liguro-Provençal and Tyrrhenian basins discussed here.

McWilliams (2008) discussed the influence of rotation on the ocean sub-mesoscale dynamics. Considering systems where strong rotation and stratification co-occur (i.e. Ro, Fr $\ll 1$), energy is thought to be transferred either downward to the smaller scales or upward to the larger scales (i.e. the inverse energy cascade hypothesis). The author also argues that these transfers often occur at the "borderlands" of fronts and currents en route to dissipation. The phenomenon of high-energy activity at frontal systems is often denominated "frontogenesis", where coherent sub-mesoscale eddy activity predominates. The kinetic energy spectrum (see Fig. 11) is often used to help diagnose the energy transfers. In the inertial energy range it is proportional to [$k = -3$], if energy is transferred forward (towards smaller scales) whereas if it is proportional to [$k = -5/3$], it behaves as an inverse energy cascade (i.e. transferred from smaller to





OSD
9, 3521–3566, 2012

larger scales). In the kinetic energy spectra of the Liguro-Provençal (red line in Fig. 11) and the Tyrrhenian basins (black line in Fig. 11) basins, both the downscale and upscale energy transfers can be depicted. However, for the Tyrrhenian basin kinetic energy activity is slightly more energetic and the upward energy transfer depicted by the $[k = -5/3]$ occurs at larger scales, when compared to the Ligurian energy spectra. This suggests that APE to KE conversion in the Tyrrhenian basin can be used to feed the boundary current(s) whereas in the Liguro-Provençal basin is mostly used to generate sub-mesoscale eddy activity, thus creating the asymmetry between the two. Apparently "frontogenesis" behaves differently in transforming the available energy in the Ligurian Sea, when compared to the Tyrrhenian basin.

The Ligurian inner cyclonic gyre and its detachment is also depicted in the calculation of the transport from the ROMS solutions (Fig. 12). Although a cyclonic inner gyre is also present in the Tyrrhenian Sea there is more connection with the outer flow, suggested by the concentration and configuration of the stream-function isolines in the channel between Sicily and Sardinia. The Ligurian inner gyre however, is somewhat detached from the activity in the boundary LPC and in the channel between the Balearic archipelago and Sardinia. The calculation of the deep (500–2000 m) transport reveals a strong cross-gyre transport, in particularly in the Tyrrhenian Sea (11 Sv), compared to 2 Sv in the Liguro-Provençal Gyre (Fig. 12). This cross-gyre transport suggests that nutrient inputs from the Ligurian coast and/or available nutrients from intense eddy activity are expected to remain longer periods trapped in the Liguro-Provençal Gyre than they are in the Tyrrhenian Gyre. Another interesting aspect is that the cross-gyre transport is larger in the deeper sections than at the surface thus residence time of buoyant materials is longer at the surface. Flushing of the basins is most likely done in depth and attached to the eddies. Strong cross-gyre transport in the Tyrrhenian Sea, due to cascading events, was also put forward in Millot (1999) review.

Convergence with eddy merging and/or interaction is likely to occur at greater depths and in the passage between the Balearic Archipelago and Sardinia. Eddies formed from the Algerian Current are known to migrate northward (e.g. Millot, 1999) and eddies formed within the Liguro-Provençal basin and/or Tyrrhenian basins also aggregate in this passage, thus inducing the high KE signal shown in Fig. 2 and discussed previously.

Further evidences of the gyre retention mechanism induced by the Liguro-Provençal cyclonic mean circulation is shown in (Poulain et al., 2012, Fig. 1). The data is further represented in (Small et al., 2012, Fig. 7), and (Dominicis et al., 2012, Fig. 1) showing surface circulation patterns derived from SVP drifters in the Liguro-Provençal basin, coherent with our ROMS calculations for the region. During Mistral as well as non-Mistral events surface drifters were retained in the inner basin circulation. This basin circulation and retention associated with an increase in the average productivity in the region lead to the suggestion that the Ligurian Productive Pool (LPP) is often formed and maintained by the regional dynamics, which differs from the neighboring Tyrrhenian oligotrophic basin (for the most part).

### 3.4 Biological implications

An interesting implication of intense (sub)mesoscale eddy activity in a basin- and open oceanic scales is that it can contribute to the MLD variability and thus to produce biological variability in the ecosystem. A deeper mixed layer might increase phytoplankton production by supplying deep nutrients to the surface layers (Polovina et al., 1995).

Concerning biological production, the Liguro-Provençal basin is known as a region where strong spring blooms occur, dominated by a marked seasonal cycle (Arnone, 1994) while no production bloom occurs in the Tyrrhenian basin. In the Ligurian case study the working hypothesis is that not only eddies can upwell nutrients from the deeper layers, but considering their numbers and spatial arrangement eddies can indeed sustain a higher productive pool in the Liguro-Provençal basin than they can in the Tyrrhenian basin. In fact, analyzing the eddy population distribution in the surface layer in relation to the mean sea surface chlorophyll production (Fig. 13), it becomes clearer that in the boundary-current where eddies are though to be formed and considering very high turbulent and horizontal advective flow, averaged productivity is very low;





OSD
9, 3521–3566, 2012

whereas in the core of the Ligurian cyclonic gyre productivity is high and remains high for longer periods. Furthermore, the cyclonic gyre in the Tyrrhenian is not as productive, although the coastal regions in this basin show high concentration of sea surface chlorophyll. The exception is the southeastern side of Corsica with a small permanent gyre that sustains high-localized productivity. This permanent structure (known as the "Bonifacio gyre") is clearly associated with a localized upwelling phenomenon induced by westerly winds blowing through the Bonifacio strait, and it displays a seasonal variability related to the general circulation in the whole area (Artale et al., 1994; Marullo et al., 1994). As observed in AVISO (Fig. 2), the passage between the Balearic Archipelago and Sardinia shows intense surface eddy activity. In depth this region is also very populated with mesoscale eddy activity (not shown), thus suggesting some blockage of the surface outflow.

Nezlin (2004) had already emphasized a peculiar aspect of this region which, in contrast to many other marginal seas, rich in mesoscale eddy activity, the nearshore zones are poor in surface chlorophyll. The Liguro-Provençal current and the presence of mesoscale eddy activity, is reflected in the high values of KE, whereas most productivity is concentrated in the center of the basin. Retention within the Ligurian basin seems to increase the residence time of locally generated eddies, whereas in the Tyrrhenian basin, eddies are transported in a conveyor-belt like fashion by the basin's boundary current. In addition, the Tyrrhenian basin has a roughed bathymetry in the center, populated by small seamounts, this can also contribute to dissipation by friction of structures that migrate to the center of this basin.

## 4 Conclusions

In this work we used a numerical ocean circulation model (partially validated) to analyze the different population behavior of eddies in two adjacent basins: the Liguro-Provençal and Tyrrhenian basins. The results showed that the eddy populations are asymmetric. Not only eddies are produced, maintained and manifested differently, but also surface eddies differed from eddies at greater depths. In both basins surface eddy activity is mostly confined to the boundary-currents, whereas in the deeper layer most eddies are concentrated on the central-deeper part. The main difference between the two basins is the residence time of eddies: the Liguro-Provençal has a much higher concentration of intermediate and deep-water eddies compared to the adjacent Tyrrhenian basin. Both models (ROMS and MERCATOR) solutions revealed that the concentration of mesoscale eddies is higher in the Liguro-Provençal basin then in the Tyrrhenian basin. The detailed analysis conducted on the eddy population suggested that eddies concentrate between 10–200 m, in the first 10 days, tend to merge and migrate vertically with a subsequent growth in the intermediate layers. The merging and migration might occur during convective processes, which are also known to occur in the region, i.e. Gulf of Lion. The analysis also showed that most eddies lived 15–60 days at the surface while in the deeper layer they live longer (90–120 days). Another detail concerns the spatial distribution of eddies: in the surface and intermediate water anticyclonic eddies were dominant, whereas in the deeper layers (200–2000 m) cyclonic eddies were predominant.

Sea surface chlorophyll concentration derived from MODIS has shown a higher concentration of mean sea surface chlorophyll in the central part of the Liguro-Provençal basin while the adjacent Tyrrhenian basin appeared to be oligotrophic. A high resolution wind stress data was used to force the simulations which contained the signal of Mistral events. The mixed layer depth has a strong reaction to these wind events. MLD reached 150 m in the Liguro-Provençal basin whereas it remained shallower in the Tyrrhenian basin. In the case of the Liguro-Provençal basin, our hypothesis is that not only eddies can upwell nutrients from the deeper layers, but considering their numbers and spatial distribution, eddies can indeed sustain a higher productive pool in the Liguro-Provençal basin. In the core of the Ligurian cyclonic gyre, populated by eddies from the coastal margins the productivity is high, while in the high turbulent boundary current productivity remains low.





OSD
9, 3521–3566, 2012

The study of (sub) mesoscale eddy populations in these Mediterranean sub-basins can continue to provide valuable information on the generation of water masses during convective events as well as transport mechanisms important for organisms, pollutants and other passive particles. It can also provide insights in the dynamics of biological events, with the potential of helping establish and manage natural reserves. Thus far, most regional studies in the Mediterranean sub-basins have focused on the study of the mean states and general current systems, which are no less important, nevertheless episodic events such as eddies and fronts must be mapped and studied in detail, in order to fully understand the complex regional dynamics. This study never claimed to have identified all the important structures which might occur, but it is hoped that it stimulates studies of even finer scales detailing their upscale energy propagation, as well as their role in connection of the Mediterranean as a whole.

*Acknowledgements.* We are thankful to Francesco Nencioli and colleagues for making the eddy detection algorithm available to the scientific community; to Mireno Borghini and Katrin Schroeder (CNR-ISMAR) for the collection and processing of the currentmeter data as well as for useful discussions on the NW Mediterranean Sea dynamics; and to Pierre Testor and Justin Small for their constructive comments to earlier versions of the manuscript. Travel funds were provided by CIMA Foundation, which enabled the authors to materialize this collaboration, and to CCM-UMa for hosting the visiting scientists in Madeira Island. Numerical model solutions were calculated at CIIMAR's HPC unit, constructed using Portuguese National Science Foundation (FCT) pluriannual funds (PesT-C/MAR/LA0015/2011), and from RAIA (0313-RAIA-1E) and RAIA.co projects, co-funded by INTERREG-IV and by FEDER ("Fundo Europeu de Desenvolvimento Regional"), through the POCTEP regional initiative. The altimeter products were produced by SSALTO/DUACS and distributed by AVISO with support from CNES. MODIS-Aqua data was extracted using the Giovanni on line data system, developed and maintained by the NASA GES DISC.

## References


Albérola, C., Millot, C., and Font, J.: On the seasonal and mesoscale variabilities on the northern current during the PRIMO-0 experiment in the Western Mediterranean Sea, Oceanol. Acta, 18, 163–192, 1995. 3524

André, G., Garreau, P., Garnier, V., and Fraunié, P.: Modelled variability of the sea surface circulation in the North-western Mediterranean Sea and in the Gulf of Lions, Ocean Dynam., 55, 294–308, 2005. 3524

Arnone, R.: The temporal and spatial variability of chlorophyll in the western Mediterranean, in: Seasonal and Interannual Variability of the Western Mediterranean Sea, Coastal Estuarine Studies, edited by: La Viollette, P. E., American Geophysical Union, Washington, DC, 195–225, 1994. 3538

Artale, V., Astraldi, M., Buffoni, G., and Gasparini, G. P.: Seasonal variability of gyre-scale circulation in the Northern Tyrrhenian Sea, J. Geophys. Res., 99, 14127–14137, 1994. 3539

Astraldi, M. and Gasparini, G. P.: The seasonal characteristics of the circulation in the North Mediterranean basin and their relationship with the atmospheric-climatic conditions, J. Geophys. Res., 97, 9531–9540, 1992. 3524

Baey, J. M., Renouard, D., and D'hieres, G. C.: Preliminary results about the stability of an intermediate water current, Deep-Sea Res. Pt. I, 42, 2063–2073, 1995. 3523

Birol, F., Cancet, M., and Estournel, C.: Aspects of the seasonal variability of the northern current (NW Mediterranean Sea) observed by altimetry, J. Marine Syst., 81, 297–311, 2010. 3524

Carniel, S., Umgiesser, G., and Sclavo, M.: Tracking the drift of a human body in the coastal ocean using numerical prediction models of the oceanic, atmospheric and wave conditions, 42, Sci. Justice, 143–151, doi:10.1016/S1355-0306(02)71819-4, 2002. 3531

Casella, E., Molcard, A., and Provenzale, A.: Mesoscale vortices in the Ligurian Sea and their effect on coastal upwelling processes, J. Marine Syst., 88, 12–19, 2011. 3528

Castellón, A., Font, J., and García, E.: The Liguro–Provençal–Catalan current, Sci. Mar., 54, 269–276, 1990. 3524

Chaigneau, A., Gizolme, A., and Grados, C.: Mesoscale eddies off Peru in altimeter records: identification algorithms and eddy spatio-temporal patterns, Prog. Oceanogr., 79, 106–119, 2008. 3528

Chelton, D. B., Schlax, M. G., Samelson, R. M., and de Szoeke, R. A.: Global observations of large oceanic eddies, Geophys. Res. Lett., 34, L15606, doi:10.1029/2007GL030812, 2007. 3528
Chelton, D. B., Schlax, M. G., and Samelson, R. M.: Global observations of nonlinear mesoscale eddies, Prog. Oceanogr., 91, 167–216, 2011. 3523
Conan, P. and Millot, C.: Variability of the northern current off Marseilles, Western Mediterranean Sea: from February to June 1992, Oceanol. Acta, 18, 193–205, 1995. 3524
da Silva, A. M., Young, C. C., and Levitus, S.: Atlas of surface marine data 1994, vol. 1, Algorithms and procedures, Tech. rep., NOAA Atlas NESDIS 6. US Gov. Printing Office, Wash., DC, 1994. 3527
Demirov, E. and Pinardi, N.: On the relationship between the water mass pathways and eddy variability in the Western Mediterranean Sea, J. Geophys. Res., 112, C02024, doi:10.1029/2005JC003174, 2007. 3534
Doglioli, A. M., Blanke, B., Speich, S., and Lapeyre, G.: Tracking coherent structures in a regional ocean model with wavelet analysis: application to Cape basin eddies, J. Geophys. Res., 112, C05043, doi:10.1029/2006JC003952, 2007. 3528
Dominicis, M., Leuzzi, G., Monti, P., Pinardi, N., and Poulain, P.-M.: Eddy diffusivity derived from drifter data for dispersion model applications, Ocean Dynam., 62, 1381–1398, 2012. 3538
Doms, G. and Schättler, U.: A Description of the Nonhydrostatic Regional Model LM, Part I: Dynamics and Numerics, Deutscher Wetterdienst, Offenbach, 2002. 3527
Dong, C., Lin, X., Liu, Y., Nencioli, F., Chao, Y., Guan, Y., Chen, D., Dickey, T., and McWilliams, J. C.: Three-dimensional oceanic eddy analysis in the Southern California Bight from a numerical product, J. Geophys. Res., 117, C00H14, doi:10.1029/2011JC007354, 2012. 3528
Ducet, N., Le Traon, P. Y., and Reverdin, G.: Global high-resolution mapping of ocean circulation from TOPEX/Poseidon and ERS-1 and -2, J. Geophys. Res., 105, 19477–19498, 2000. 3525
Echevin, V., Crépon, M., and Mortier, L.: Simulation and analysis of the mesoscale circulation in the northwestern Mediterranean Sea, Ann. Geophys., 21, 281–297, doi:10.5194/angeo-21-281-2003, 2003. 3523, 3524
Font, J., Salat, J., and Tintoré, J.: Permanent features of the circulation in the Catalan Sea, Oceanol. Acta, 9, 51–57, 1988. 3524
Gasparini, G. P., Zodiatis, G., Astraldi, M., Galli, C., and Sparnocchia, S.: Winter intermediate water lenses in the Ligurian Sea, J. Marine Syst., 20, 319–332, 1999. 3523





OSD
9, 3521–3566, 2012
Eddy populations in adjacent basins
R. M. A. Caldeira et al.

Grilli, F. and Pinardi, N.: The computation of Rossby radii of deformation for the Mediterranean Sea, MTP News, 6, 4, 1998. 3527

Herbaut, C., Martel, F., and Crépon, M.: A sensitivity study of the general circulation of the wEstern Mediterranean Sea. Part II: The response to atmospheric forcing, J. Phys. Oceanogr., 27, 2126–2145, 1997. 3531

Isern-Fontanet, J., Font, J., García-Ladona, E., Emelianov, M., Millot, C., and Taupier-Letage, I.: Spatial structure of anticyclonic eddies in the Algerian basin (Mediterranean Sea) analyzed using the Okubo–Weiss parameter, Deep-Sea Res.Pt. II, 51, 3009–3028, 2004. 3528

Legg, S. and McWilliams, J. C.: Convective modifications of a geostrophic eddy field, J. Phys. Oceanogr., 31, 874–891, 2001. 3534

Liu, Y., Dong, C., Guan, Y., Chen, D., McWilliams, J., and Nencioli, F.: Eddy analysis in the subtropical zonal band of the North Pacific Ocean, Deep-Sea Res. Pt I, 68, 54–67, 2012. 3528

Marullo, S., Santoleri, R., and Bignami, F.: The surface characteristics of the Tyrrhenian Sea: historical satellite data analysis, in: Seasonal and Interannual Variability of the Western Mediterranean Sea, Coastal Estuarine Stud., edited by: La Viollette, P. E., American Geophysical Union, Washington, DC, 135–154, 1994. 3523, 3539

McWilliams, J. C.: Fluid dynamics at the margin of rotational control, Environ. Fluid Mech., 8, 441–449, 2008. 3536

Millot, C.: Circulation in the Western Mediterranean Sea, J. Marine Syst., 20, 423–442, 1999. 3523, 3524, 3525, 3529, 3530, 3537

Millot, C. and Taupier-Letage, I.: Circulation in the Mediterranean Sea, in: Handbook of Environmental Chemistry, edited by: Saliot, A., Springer-Verlag, Berlin, Heidelberg, 29–66, 2005. 3523

Molcard, A. J., Pinardi, N., and Ansaloni, R.: A spectral element ocean model on the cray T3D: the interannual variability of the Mediterranean Sea general circulation, Phys. Chem. Earth, 23, 491–495, 1998. 3528

Molcard, A., Pinardi, N., Iskandarani, M., and Haidvogel, D. B.: Wind driven general circulation of the Mediterranean Sea simulated with a Spectral Element Ocean Model, Dynam. Atmos. Oceans, 35, 97–130, 2002. 3528

Montani, A., Marsigli, C., Nerozzi, F., Paccagnella, T., Tibaldi, S., and Buizza, R.: The Soverato flood in Southern Italy: performance of global and limited-area ensemble forecasts, Nonlinear Proc. Geoph., 10, 261–274, 2003. 3527

Nencioli, F., Dong, C., Dickey, T., Washburn, L., and McWilliams, J. C.: A vector geometry-based eddy detection algorithm and its application to a high-resolution numerical model product and high-frequency radar surface velocities in the Southern California Bight, J. Atmos. Ocean. Tech., 27, 564–579, 2010. 3528

Nezlin, N. P.: Remotely sensed seasonal dynamics of phytoplankton in the Ligurian Sea in 1997–1999, J. Geophys. Res., 109, C07013, doi:10.1029/2000JC000628, 2004. 3539

Pascual, A., Pujol, M. I., Larnicol, G., Le Traon, P. Y., and Rio, M. H.: Mesoscale mapping capabilities of multisatellite altimeter missions: first results with real data in the Mediterranean Sea, J. Marine Syst., 65, 190–211, 2007. 3525

Pedlosky, J., Pratt, L. J., Spall, M. A., and Helfrich, K.: Circulation around islands and ridges, J. Mar. Res., 55, 1199–1251, 1997. 3535, 3536

Pinardi, N. and Masetti, E.: Variability of the large scale general circulation of the Mediterranean Sea from observations and modelling: a review, Palaeogeogr., Palaeocl., 158, 153–173, 2000. 3523

Pinardi, N. and Navarra, A.: Baroclinic wind adjustment processes in the Mediterranean Sea, Deep-Sea Res. Pt. II, 40, 1299–1326, 1993. 3527

Pinot, J.-M., Tintoré, J., and Gomis, D.: Multivariate analysis of the surface circulation in the Balearic Sea, Prog. Oceanogr., 36, 343–376, 1995. 3524

Polovina, J. J., Mitchum, G. T., and Evans, G. T.: Decadal and basin-scale variation in mixed layer depth and the impact on biological production in the Central and North Pacific, 1960–88, Deep-Sea Res. Pt. I, 42, 1701–1716, 1995. 3538

Poulain, P. M., Gerin, R., Rixen, M., Zanasca, P., Teixeira, J., Griffa, A., Molcard, A., De Marte, M., and Pinardi, N.: Aspects of the surface circulation in the Liguro-Provençal basin and Gulf of Lion as observed by satellite-tracked drifters (2007–2009), B. Geofis. Teor. Appl., 53, 261–279, 2012. 3531, 3538

Rio, M. H. and Hernandez, F.: A mean dynamic topography computed over the world ocean from altimetry, in situ measurements, and a geoid model, J. Geophys. Res., 109, C12032, doi:10.1029/2003JC002226, 2004. 3525

Robinson, A. R., Leslie, W. G., Theocharis, A., and Lascaratos, A.: Mediterranean sea circulation, in: Ocean Currents: A Derivative of the Encyclopedia of Ocean Sciences, edited by: Steele, J. H., Thorpe, S. A., and Turekian, K. K., Academic Press, San Diego, 1689–1705, 2001. 3523, 3524

Sadarjoen, A. I. and Post, F. H.: Detection, quantification, and tracking of vortices using streamline geometry, Comput. Graph., 24, 333–341, 2000. 3528

Salat, J.: The interaction between the Catalan and Balearic currents in the Southern Catalan Sea, Oceanol. Acta, 18, 227–234, 1995. 3524

Sammari, C., Millot, C., and Prieur, L.: Aspects of the seasonal and mesoscale variabilities of the northern current in the Western Mediterranean Sea inferred from the PROLIG-2 and PROS-6 experiments, Deep-Sea Res- Pt. I, 42, 893–917, 1995. 3523, 3524

Santoleri, R., Salusti, E., and Stocchino, C.: Hydrological currents in the Ligurian Sea, Nuovo Cimento C, 6, 353–370, 1983. 3523

Schroeder, K., Taillandier, V., Vetrano, A., and Gasparini, G. P.: The circulation of the Western Mediterranean Sea in spring 2005 as inferred from observations and from model outputs, Deep-Sea Res. Pt. I, 55, 947–965, 2008. 3531

Shchepetkin, A. F.: A method for computing horizontal pressure-gradient force in an oceanic model with a nonaligned vertical coordinate, J. Geophys. Res., 108, 3090, doi:10.1029/2001JC001047, 2003. 3527

Shchepetkin, A. F. and McWilliams, J. C.: The regional oceanic modeling system (ROMS): a split-explicit, free-surface, topography-following-coordinate oceanic model, Ocean Model., 9, 347–404, 2005. 3527

Small, R. J., Carniel, S., Campbell, T., Teixeira, J., and Allard, R.: The response of the Ligurian and Tyrrhenian Seas to a summer Mistral event: a coupled atmosphere–ocean approach, Ocean Model., 48, 30–44, 2012. 3524, 3529, 3530, 3531, 3538

Steppeler, J., Hess, R., Schättler, U., and Bonaventura, L.: Review of numerical methods for nonhydrostatic weather prediction models, Meteorol. Atmos. Phys., 82, 287–301, 2003. 3527

Taupier-Letage, I. and Millot, C.: General hydrodynamical features in the Ligurian Sea inferred from the DYOME experiment, Oceanol. Acta, 9, 119–131, 1986. 3524

Testor, P. and Gascard, J. C.: Large-scale spreading of deep waters in the Western Mediterranean Sea by submesoscale coherent eddies, J. Phys. Oceanogr., 33, 75–87, 2003. 3531

Testor, P. and Gascard, J. C.: Large scale flow separation and mesoscale eddy formation in the Algerian basin, Prog. Oceanogr., 66, 211–230, 2005. 3531

Testor, P. and Gascard, J. C.: Post-convection spreading phase in the Northwestern Mediterranean Sea, Deep-Sea Res. Pt. I, 53, 869–893, 2006. 3531

Vetrano, A.: Water flux estimates in the central Mediterranean Sea from an inverse box model, J. Geophys. Res., 109, C01019, doi:10.1029/2003JC001903, 2004. 3524

Vignudelli, S., Cipollini, P., Astraldi, M., Gasparini, G. P., and Manzella, G.: Integrated use of altimeter and in situ data for understanding the water exchanges between the Tyrrhenian and Ligurian Seas, J. Geophys. Res., 105, 19649–19663, 2000. 3524

Zavatarelli, M. and Mellor, G. L.: A numerical study of the Mediterranean Sea circulation, J. Phys. Oceanogr., 25, 1384–1414, 1995. 3523





OSD

9, 3521–3566, 2012

Eddy populations in adjacent basins

R. M. A. Caldeira et al.

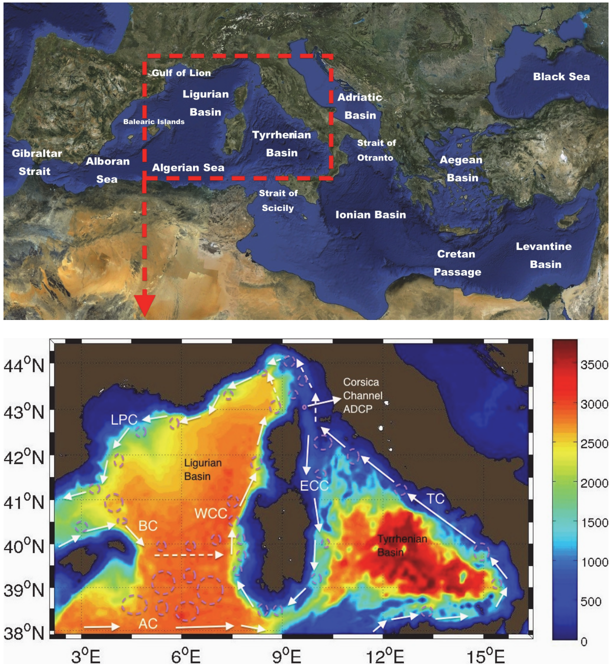


**Fig. 1.** Maps showing the (upper panel) sub-basin structure of the Mediterranean Sea; (lower panel) bathymetry (meters) of the West Mediterranean Sea sub-basins: Tyrrhenian and Liguro-Provençal. The approximate location of the Corsica Channel ADCP is also shown (purple dot). The region in the lower panel is also representative of the ROMS numerical domain. The arrows summarize the surface dynamics of the region; purple round structures represent eddies and dashed lines less permanent structures. The labels represent: TC – Tyrrhenian Current; ECC – Eastern Corsica Current; WCC – Western Corsica Current; LPC – Ligurian-Provençal Current; BC – Balearic Current; AC – Algerian Current.



OSD
9, 3521–3566, 2012

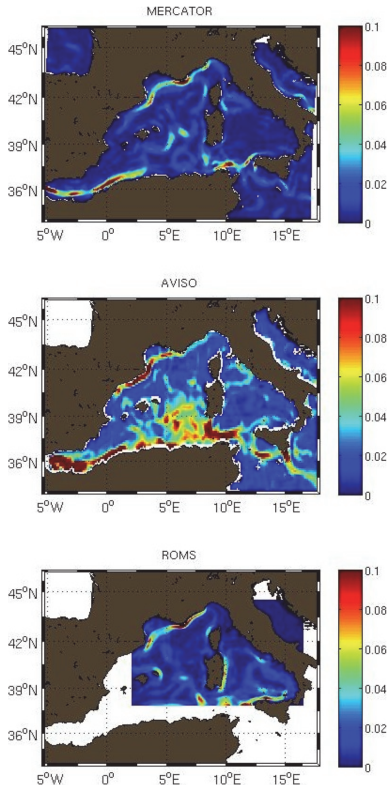


**Fig. 2.** Mean Kinetic Energy, derived from sea surface velocity for 2009, from (i) MERCATOR (upper panel); (ii) AVISO (middle panel); (iii) ROMS (bottom panel). Similar patterns were obtained for 2010 (not shown).



OSD
9, 3521–3566, 2012

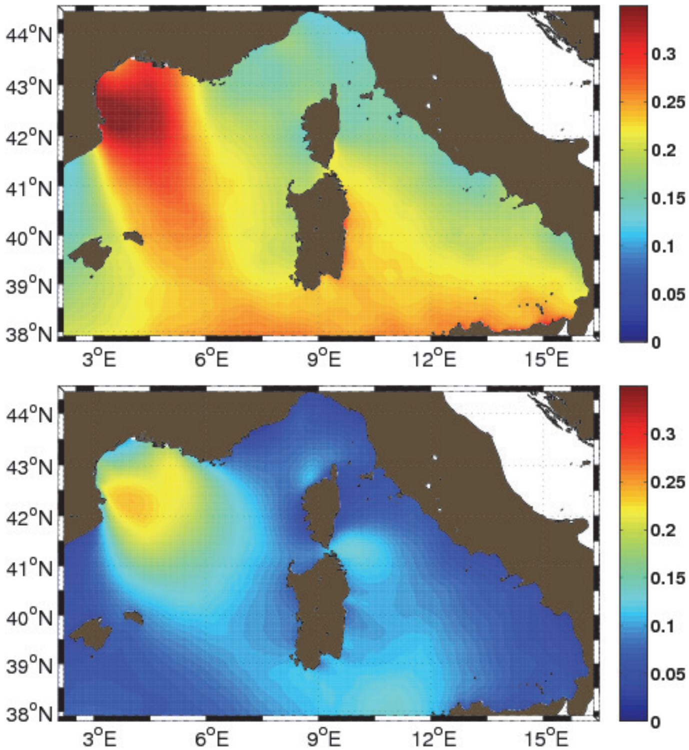


**Fig. 3a.** Mean wind stress showing the strong signature of the Mistral wind events from the COSMO-I7 atmospheric forcing for summer (upper panel) winter (bottom panel) of 2009.



OSD
9, 3521–3566, 2012
Eddy populations in adjacent basins
R. M. A. Caldeira et al.

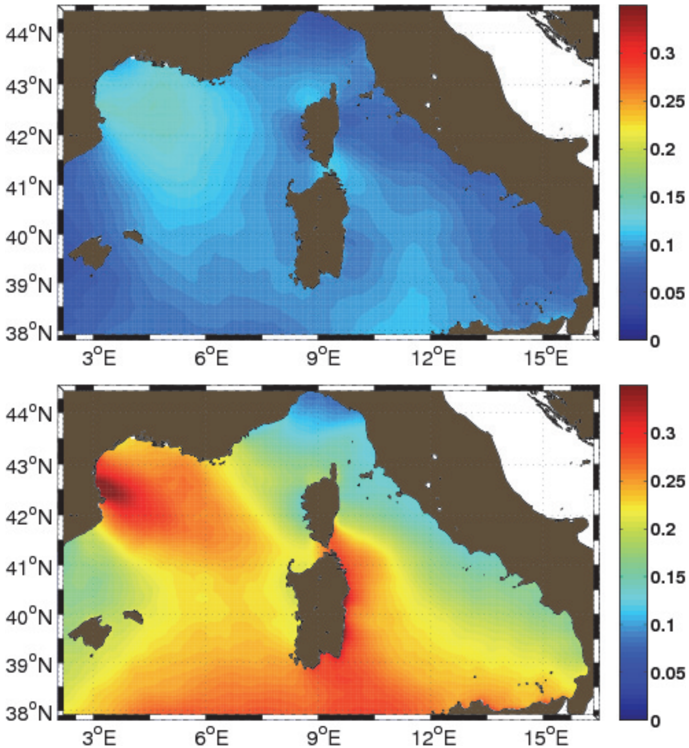


**Fig. 3b.** Continued. Summer (upper panel) winter (bottom panel) of 2010.





OSD
9, 3521–3566, 2012

Eddy populations in adjacent basins

R. M. A. Caldeira et al.

Title Page
Abstract
Introduction
Conclusions
References
Tables
Figures
◀
▶
Back
Close
Full Screen / Esc
Printer-friendly Version
Interactive Discussion

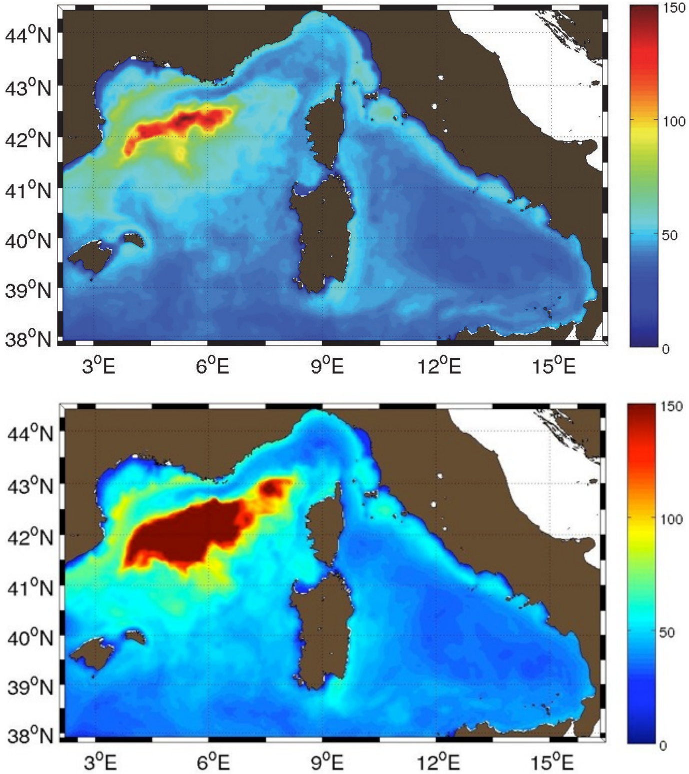


**Fig. 4.** Yearly mean Mixed Layer Depth in meters (MLD) calculated from ROMS solutions showing strong convection induced by the strong mistral events, leeward of the Gulf of Lion (upper panel) 2009; (lower panel) 2010.





OSD
9, 3521–3566, 2012

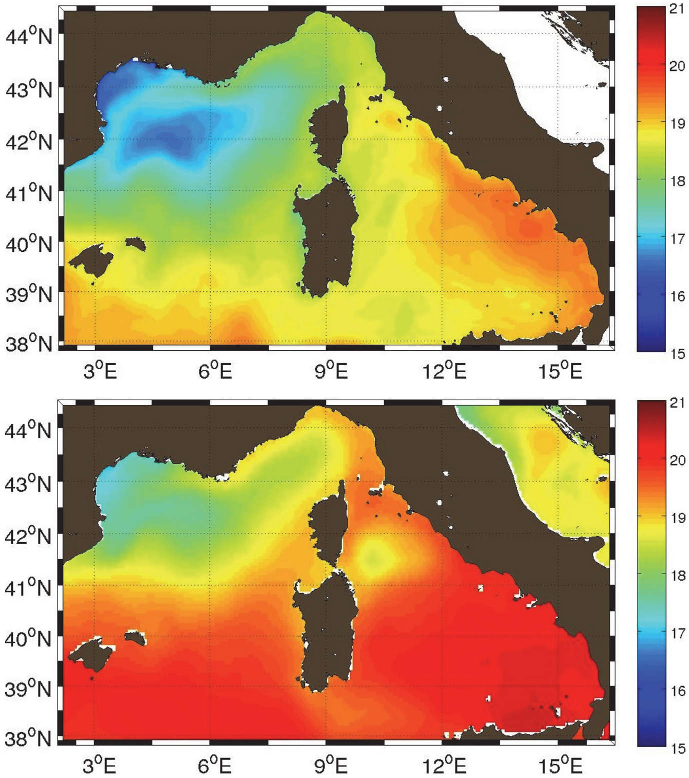


**Fig. 5a.** SST mean field for 2009 (upper panel) ROMS SST mean; (bottom panel) GOS-SST mean; and a strong thermal gradient between the Liguria and the outer-basin is shown in all plots (between Balearic Archipelago and Sardinia).





OSD
9, 3521–3566, 2012

Eddy populations in adjacent basins

R. M. A. Caldeira et al.

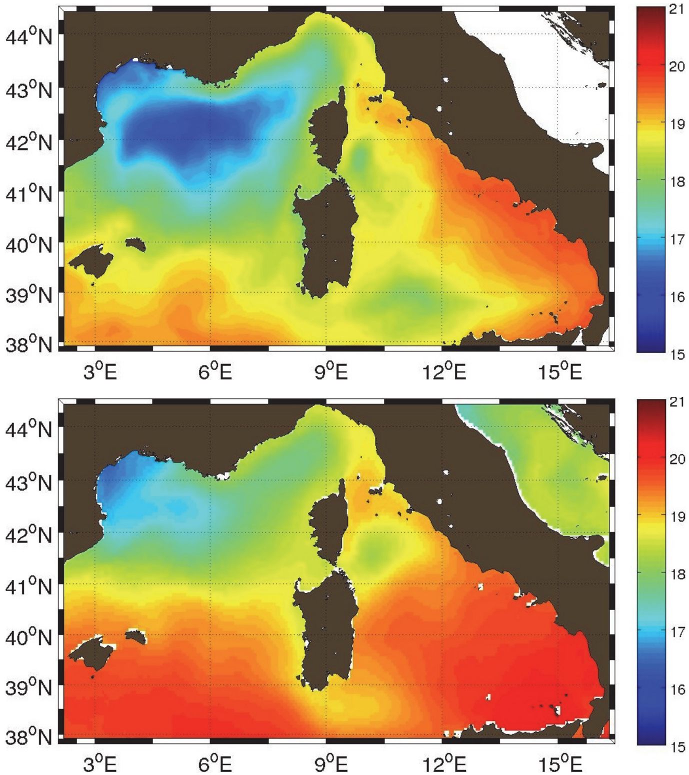


**Fig. 5b.** Continued. 2010: (upper panel) ROMS SST mean; (lower panel) GOS-SST mean.





OSD
9, 3521–3566, 2012

Eddy populations in adjacent basins

R. M. A. Caldeira et al.

Title Page
Abstract
Introduction
Conclusions
References
Tables
Figures
◀|
|▶
◀
▶
Back
Close
Full Screen / Esc
Printer-friendly Version
Interactive Discussion

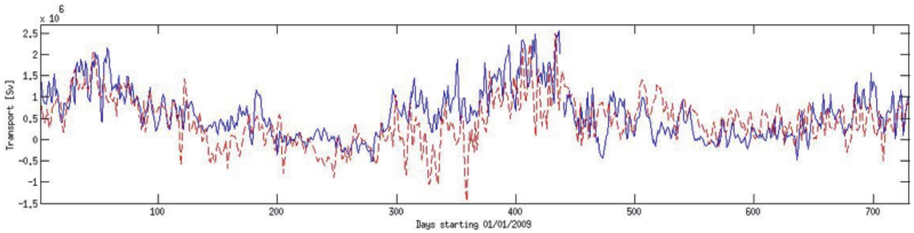


**Fig. 6.** Time-series (2009–2010) of transport in the Corsica Channel. Red dashed line: transport derived from moored current meters. Blue continuous line: transport calculated from ROMS solutions for the same period from the approximately same location.

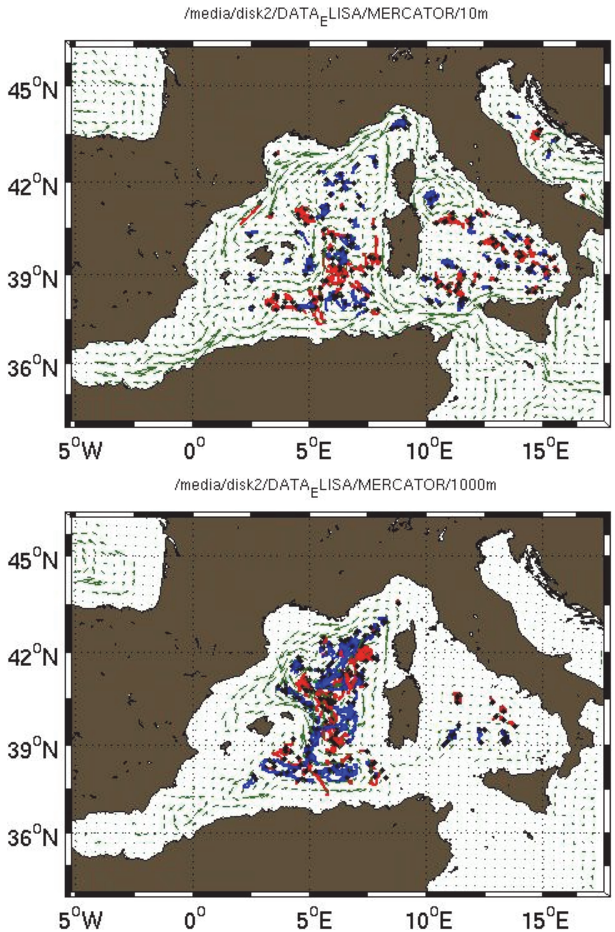


**Fig. 7a.** Detected eddies with lifetimes greater than 10 days for the two year (2009–2010) numerical solutions in: MERCATOR at 10 (upper panel) and 500 m depth (bottom panel); blue lines represent cyclonic eddies and red lines represent anticyclonic eddies.





OSD
9, 3521–3566, 2012

Eddy populations in adjacent basins

R. M. A. Caldeira et al.

Title Page
Abstract Introduction
Conclusions References
Tables Figures
◀I ▶I
◀ ▶
Back Close
Full Screen / Esc
Printer-friendly Version
Interactive Discussion

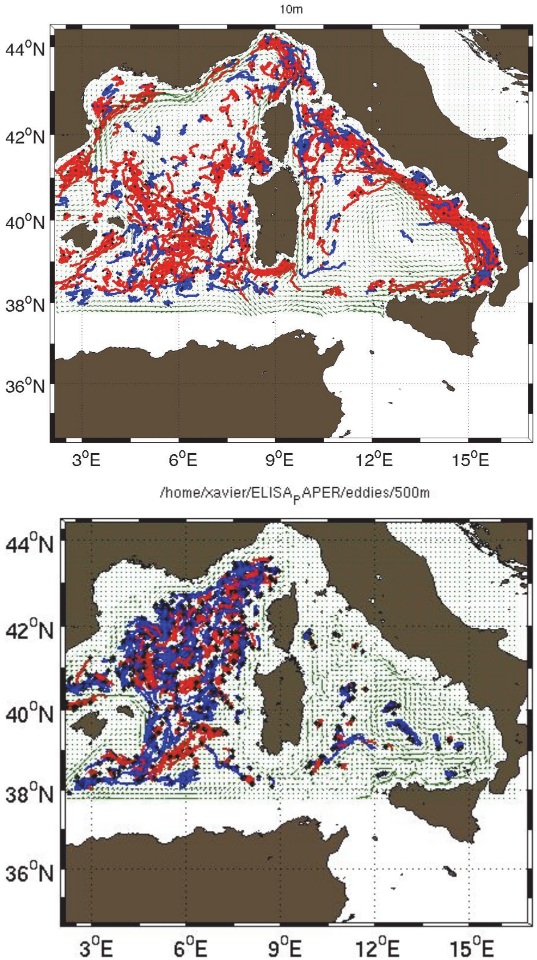


**Fig. 7b.** Continued. ROMS at 10 m (upper panel), 500 m (bottom panel). Blue lines represent cyclonic eddies and red lines represent anticyclonic eddies.





OSD
9, 3521–3566, 2012

Eddy populations in adjacent basins

R. M. A. Caldeira et al.

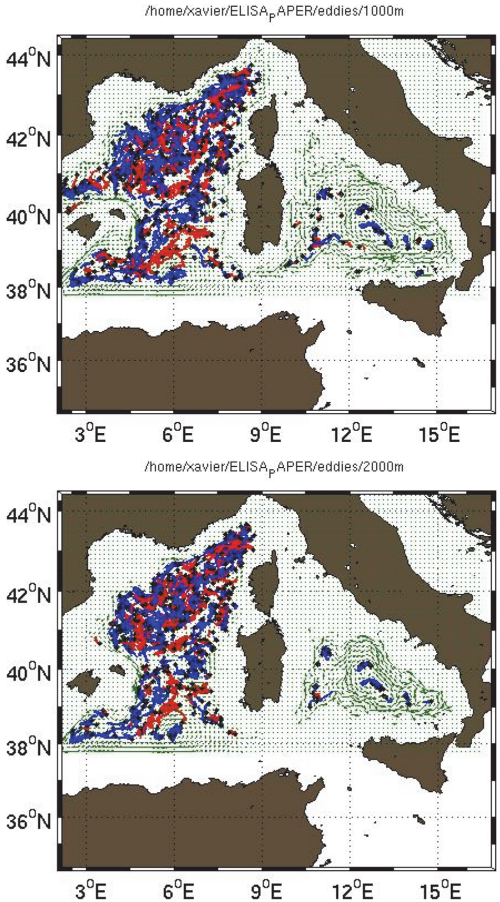


**Fig. 7c.** Continued. ROMS at 1000 m (upper panel) and 2000 m depth (bottom panel). Blue lines represent cyclonic eddies and red lines represent anticyclonic eddies.





OSD
9, 3521–3566, 2012

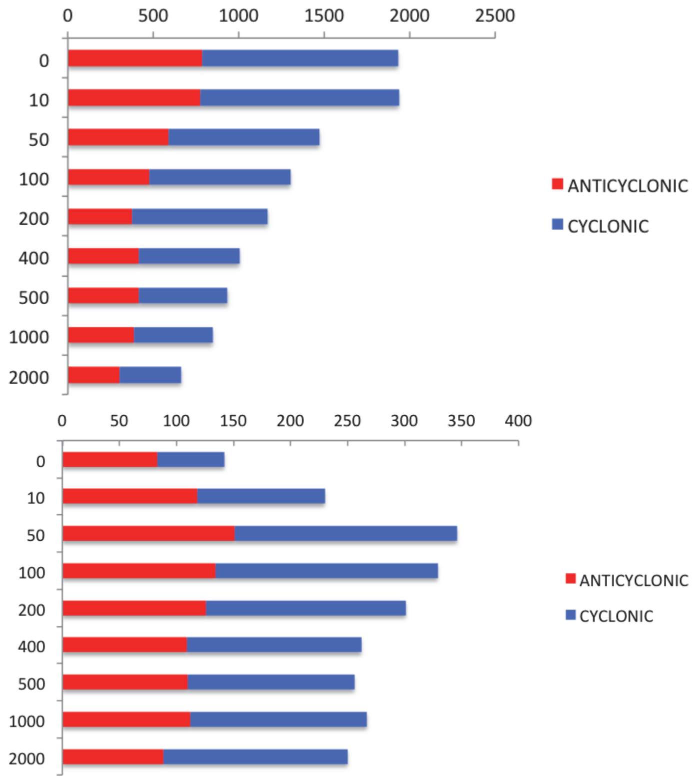


**Fig. 8a.** Depth distribution of eddies (2009–2010) with lifetimes 1 to 10 days for MERCATOR (top panel); greater than 10 days for MERCATOR (bottom panel). Red bars represent anticyclonic and blue bars, cyclonic eddies.





OSD
9, 3521–3566, 2012

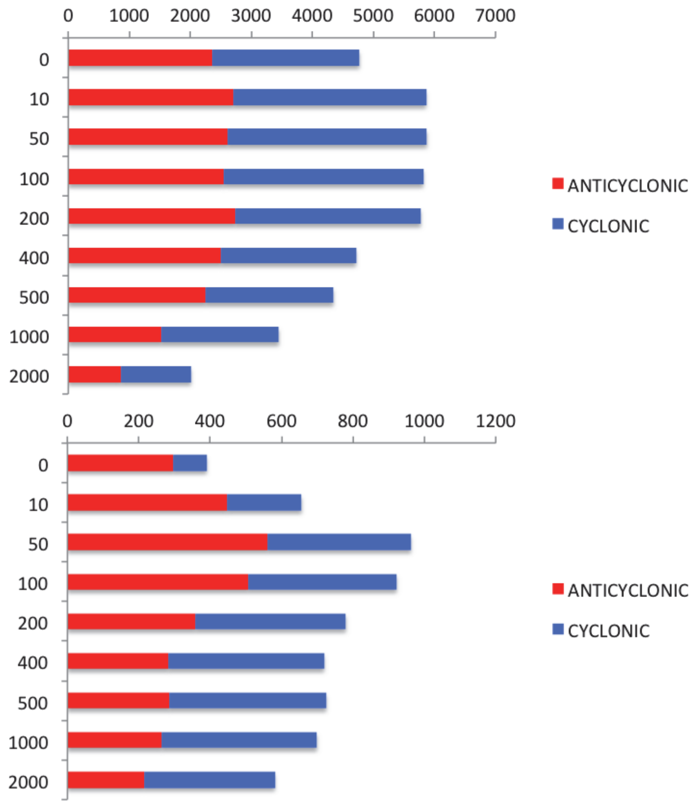


**Fig. 8b.** Continued. 1 to 10 days for ROMS (top panel); and greater than 10 days for ROMS (bottom panel). Red bars represent anticyclonic and blue bars, cyclonic eddies.





OSD
9, 3521–3566, 2012

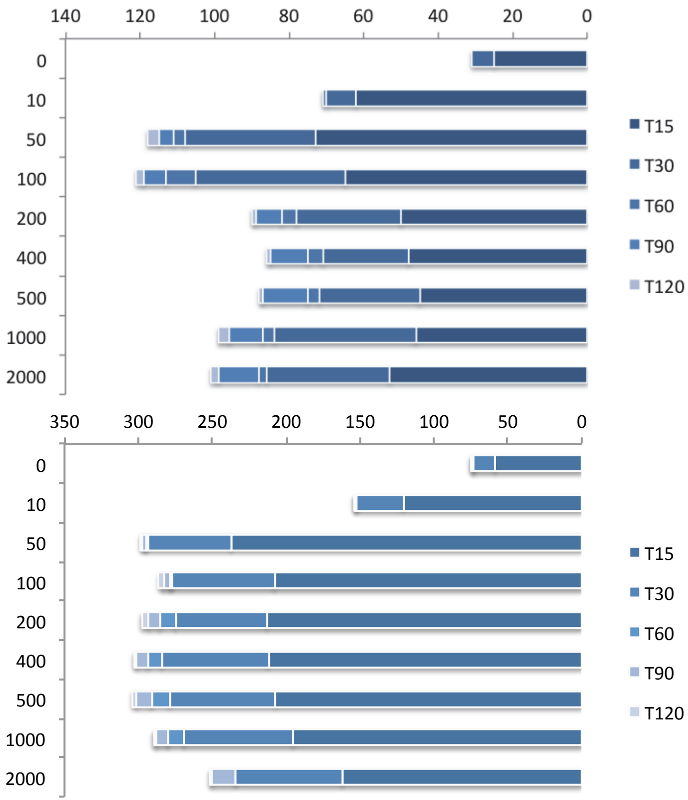


**Fig. 9a.** Depth distribution (0–2000 m) of the cyclonic eddies (2009, 2010) for different lifetime periods: T15: 10–15 days; T30: 16–30 days; T60: 31–60 days; T90: 61–90 days; T120: 91–120 days. MERCATOR (top panel) and ROMS cyclonic eddies (bottom panel).





OSD
9, 3521–3566, 2012

Eddy populations in adjacent basins

R. M. A. Caldeira et al.

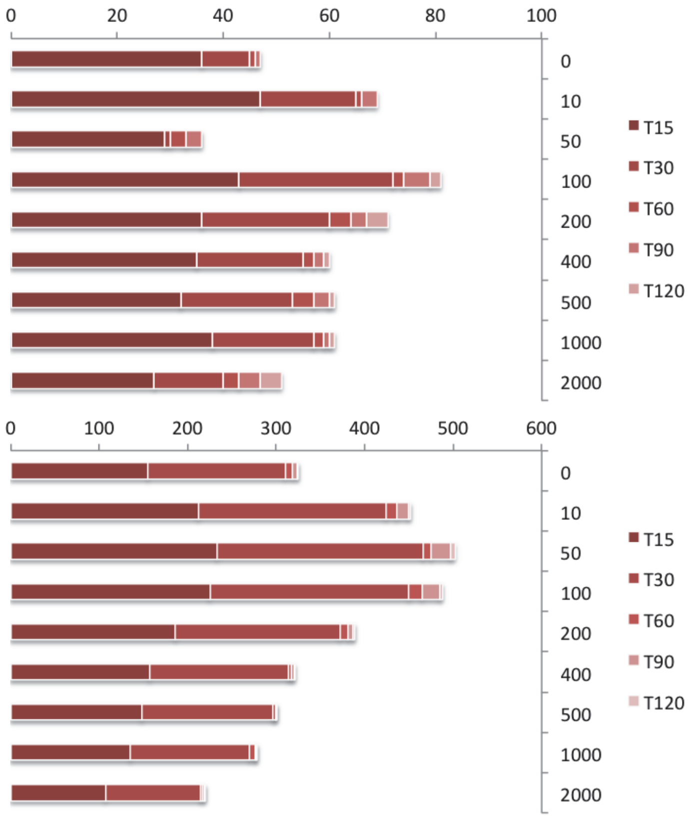


**Fig. 9b.** Anticyclonic eddies detected in MERCATOR (top panel) and ROMS (bottom panel), solutions.



OSD

9, 3521–3566, 2012

Eddy populations in adjacent basins

R. M. A. Caldeira et al.

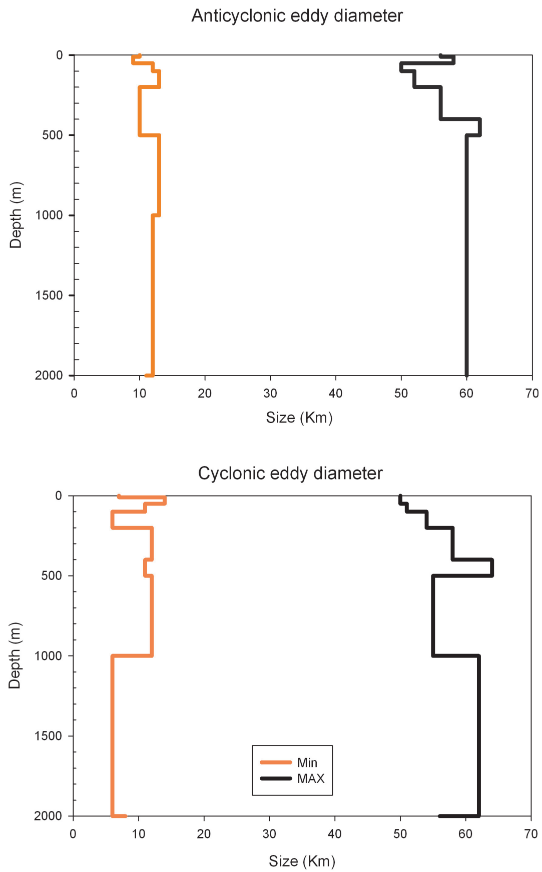


**Fig. 10.** Minimum and maximum eddy-size as a function of depth derived from ROMS 2009–2010 calculation. Anticyclone eddies represented in the upper panel whereas cyclonic eddies are represented in the lower panel.





OSD
9, 3521–3566, 2012
Eddy populations in adjacent basins
R. M. A. Caldeira et al.

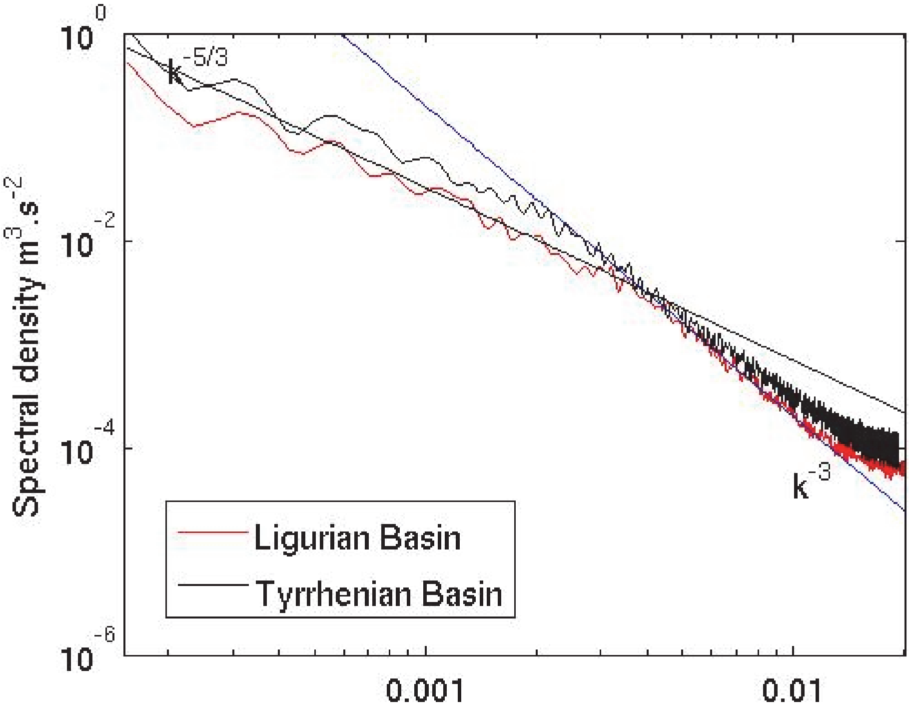


**Fig. 11.** Kinetic energy spectra as a function of horizontal wave number magnitude. A power-law proportional to $k^{-5/3}$ (black) and to $k^{-3}$ (blue) is shown for reference. Spectra in the Tyrrhenian basin is represented in black, whereas the red line represents the spectra in the Ligurian basin.





OSD
9, 3521–3566, 2012

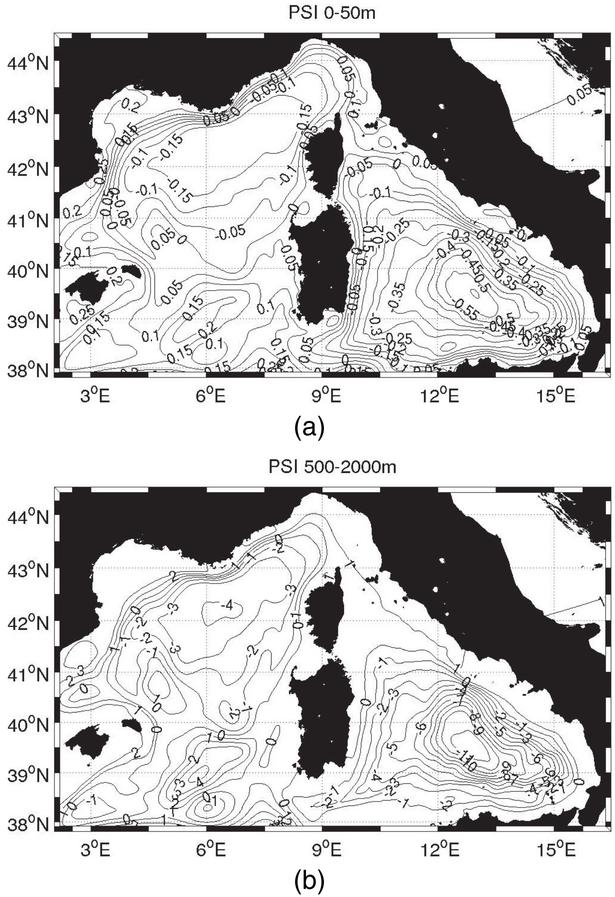


**Fig. 12.** Transport (SV) derived from ROMS solutions (2009–2010) for: **(a)** surface 0–50m: **(b)** 500–2000 m.

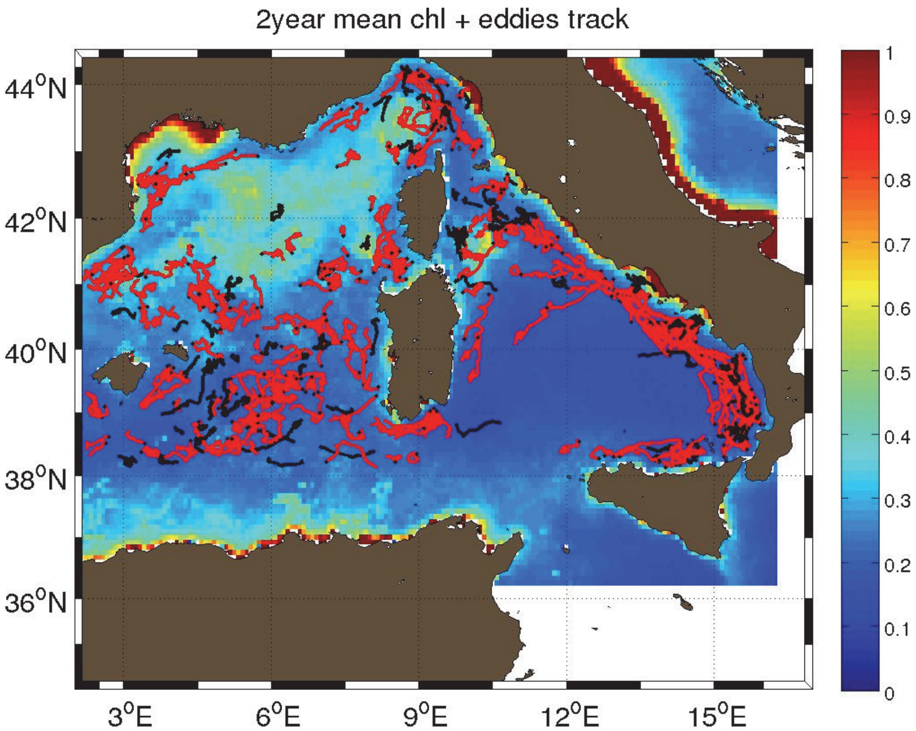


**Fig. 13.** MODIS derived mean chlorophyll with overlaid eddy trajectories at 10 m, for 2009–2010.





OSD
9, 3521–3566, 2012

Eddy populations in adjacent basins

R. M. A. Caldeira et al.

Title Page
Abstract | Introduction
Conclusions | References
Tables | Figures
◀| |▶
◀ ▶
Back | Close
Full Screen / Esc
Printer-friendly Version
Interactive Discussion